

NEW TECHNOLOGICAL DEVELOPMENT FOR FAR INFRARED BOLOMETER ARRAYS

E.Mottin, Patrick Agnese, E.Peytavit, A.Beguin, P.Rey
LETI/CEA.G, 17 Avenue des Martyrs, 38054 GRENOBLE Cedex 9, France

ABSTRACT

Since 1997, CEA/SAP and CEA/LETI/SLIR have been developing monolithic Si bolometer arrays sensitive in the far infrared and submillimeter range for space observations. Two focal planes, 32x64 and 16x32 pixel arrays, are designed and manufactured for the PACS (Photodetector Array Camera and Spectrometer) instrument of the Herschel observatory, to be launched in 2007. The two arrays cover respectively the 60-130 μm and 130-210 μm ranges. The goal of these large bolometer arrays is to achieve observations in a Background limited NEP around $10^{-16} \text{ W.Hz}^{-1/2}$. The detector physics and manufacture techniques of the different stages of these arrays are first presented. Then we describe the read-out and multiplexing cold electronics (300mK) that make possible several functional modes (temporal and fixed pattern noise reduction,...). The latest experimental measurements carried out with the complete detector system at the nominal temperature are presented and performances are discussed.

1. INTRODUCTION

The ‘Herschel Space Observatory’, to be launched by the European Space Agency in 2007, will perform imaging photometry and spectroscopy in the far-infrared and sub-millimetre spectrum. Its superfluid helium cryostat houses three instruments (ref [1]& [2]), the Photodetector Array Camera and Spectrometer (PACS), the Spectral and Photometric Imaging Receiver (SPIRE) and the Heterodyne Instrument for the Far Infrared (HIFI). The PACS photometer channel comprises two focal planes, 32x64 and 16x32 pixel arrays, that CEA/DSM/DAPNIA/Service d’Astrophysique and CEA/DRT/LETI/DOPT/SLaboratoire d’InfraRouge have designed and are manufacturing (ref [3]).

The focal planes design is based on a new bolometer arrays technology developed and optimized for the Herschel mission since 1997. At the end of 1999, a fully operational 16x16 pixels detector was complete, and optimized for 350 μm wavelength absorption range. Since then, the 1999 design has been upgraded and optimized in order to meet the PACS requirements:

- The Photometer is composed of sub units of 256 active pixels. It is divided into two Bolometer Focal Planes (BFP), one covering the 60-130 μm range, called ‘blue’ BFP, composed of 4 x 2 sub-arrays of 16 x 16 pixels tiled together, and one 130-210 μm ‘red’ BFP formed by 2 sub-arrays of 16 x 16 pixels.
- The goal of a Noise Equivalent Power (NEP) around $10^{-16} \text{ W.Hz}^{-1/2}$ in the high background conditions (a few pW per pixel) is achieved by using high impedance thermometers associated to CMOS read-out electronics circuits cooled at 300 mK.

It was required to multiplex the pixel outputs by a large factor (goal 1->1) to limit the amount of electronics channels to be implemented in a space application. We describe hereafter the advantages and drawbacks of the adopted solution.

The first PACS detector array was achieved in January 2002. A complete assembly (with 6 functional sub arrays out of 10) was delivered to the Max Planck Institute in April 2004 for integration in the QM instrument.

2. DETECTOR DESIGN

The bolometers design is based on an all Silicon technology:

- 1- Thermometers are made by ion implantation and diffusion on a double SOI substrate.
- 2- The infra-red flux absorption is achieved by a vertical cavity constituted by a metallic mesh, supported by a Si grid and placed above a reflector.

Report Documentation Page				Form Approved OMB No. 0704-0188	
Public reporting burden for the collection of information is estimated to average 1 hour per response, including the time for reviewing instructions, searching existing data sources, gathering and maintaining the data needed, and completing and reviewing the collection of information. Send comments regarding this burden estimate or any other aspect of this collection of information, including suggestions for reducing this burden, to Washington Headquarters Services, Directorate for Information Operations and Reports, 1215 Jefferson Davis Highway, Suite 1204, Arlington VA 22202-4302. Respondents should be aware that notwithstanding any other provision of law, no person shall be subject to a penalty for failing to comply with a collection of information if it does not display a currently valid OMB control number.					
1. REPORT DATE 13 JUL 2005		2. REPORT TYPE N/A		3. DATES COVERED -	
4. TITLE AND SUBTITLE New Technological Development For Far Infrared Bolometer Arrays				5a. CONTRACT NUMBER	
				5b. GRANT NUMBER	
				5c. PROGRAM ELEMENT NUMBER	
6. AUTHOR(S)				5d. PROJECT NUMBER	
				5e. TASK NUMBER	
				5f. WORK UNIT NUMBER	
7. PERFORMING ORGANIZATION NAME(S) AND ADDRESS(ES) LETI/CEA.G, 17 Avenue des Martyrs, 38054 GRENOBLE Cedex 9, France				8. PERFORMING ORGANIZATION REPORT NUMBER	
9. SPONSORING/MONITORING AGENCY NAME(S) AND ADDRESS(ES)				10. SPONSOR/MONITOR'S ACRONYM(S)	
				11. SPONSOR/MONITOR'S REPORT NUMBER(S)	
12. DISTRIBUTION/AVAILABILITY STATEMENT Approved for public release, distribution unlimited					
13. SUPPLEMENTARY NOTES See also ADM001791, Potentially Disruptive Technologies and Their Impact in Space Programs Held in Marseille, France on 4-6 July 2005., The original document contains color images.					
14. ABSTRACT					
15. SUBJECT TERMS					
16. SECURITY CLASSIFICATION OF:			17. LIMITATION OF ABSTRACT UU	18. NUMBER OF PAGES 10	19a. NAME OF RESPONSIBLE PERSON
a. REPORT unclassified	b. ABSTRACT unclassified	c. THIS PAGE unclassified			

- 3- Two cold electronics stages are associated to the detector arrays and work respectively at 300mK and 2K. They consist of Si CMOS circuits.

1. Thermometer

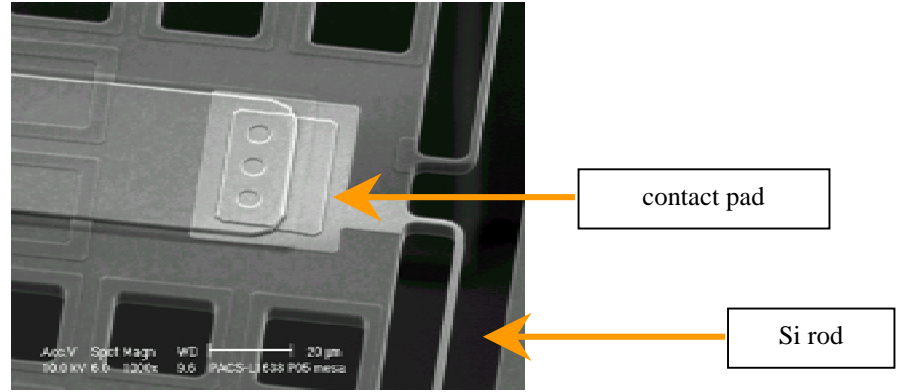


Figure 1 MESA thermometer

The problem of pixel multiplexing was solved by the use of CMOS gates, circuit already used in space application for the ISOCAM detector array [ref. 4] The excess noise introduced by this kind of electronics is overcome by a very high response, typically a few 10^{10} V/W. This response is achieved by using very high impedance thermometers, i.e. 1 to 10 G Ω resistances at 300 mK. Such resistances are obtained by a specific process of ion implantation (phosphorus and boron) on a double SOI substrate. A thermal diffusion is then applied to homogenize the implantation.

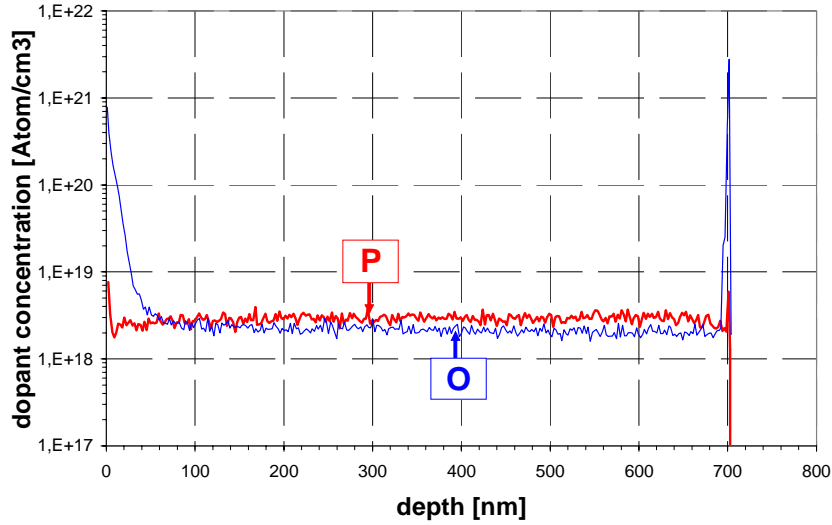


Figure 2: P & O dopants profile within the thermometer depth

Highly accurate and homogeneous ionic implantations are achieved. For example, a very homogeneous phosphorus concentration versus depth centered around 3.10^{18} atoms /cm³ was measured for a 2.10^{14} atoms/cm² dose. On Figure 2, we can distinguish at the interfaces the SiO₂/Si0.7 μ m/SiO₂ diffusion barriers. The doping reproducibility is better than 5%, which is actually on the order of the measurement accuracy.

After thermal diffusion, contact pads (Figure 1) are implanted above the thermometer and micro-etching of the thermometric layer adjusts the required geometry (dimension= 40 μ m x 600 μ m).

2. Flux absorber

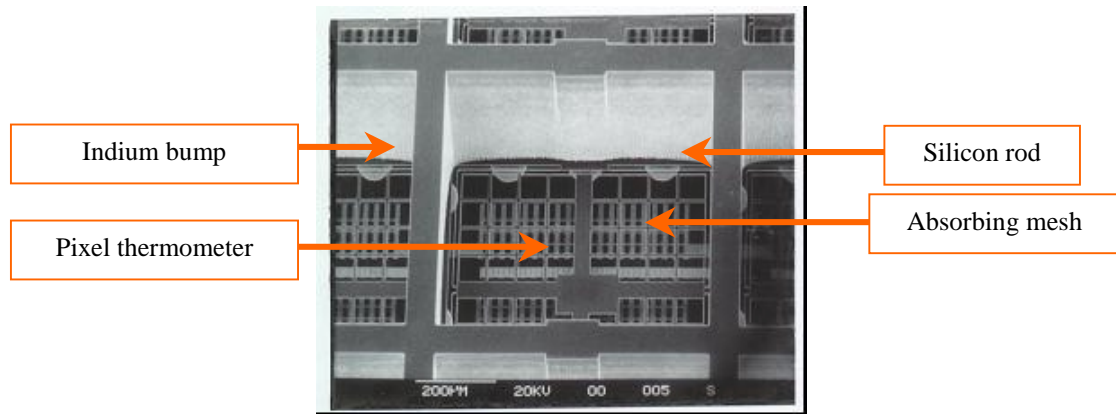


Figure 3: Picture of one pixel

High absorption of submillimeter wavelengths is achieved here by use of resonant quarter wave cavities. This process was described long time ago by Dennisson and Hadley [ref 4]. The cavity is obtained by a metallic reflector located $20/25\mu\text{m}$ below the metallic (TiN) absorbing mesh. The surface impedance of the absorber is matched to the vacuum one, allowing 100% direct theoretical efficiency. The absorber is deposited on the silicon grid ($5\mu\text{m}$ thick) containing the thermometer. The depth of the quarter wave cavity is controlled by Indium bumps diameter. These bumps ensure in addition the electric contact between detector and readout circuits, and evacuate the power absorbed or dissipated in the detector arrays.

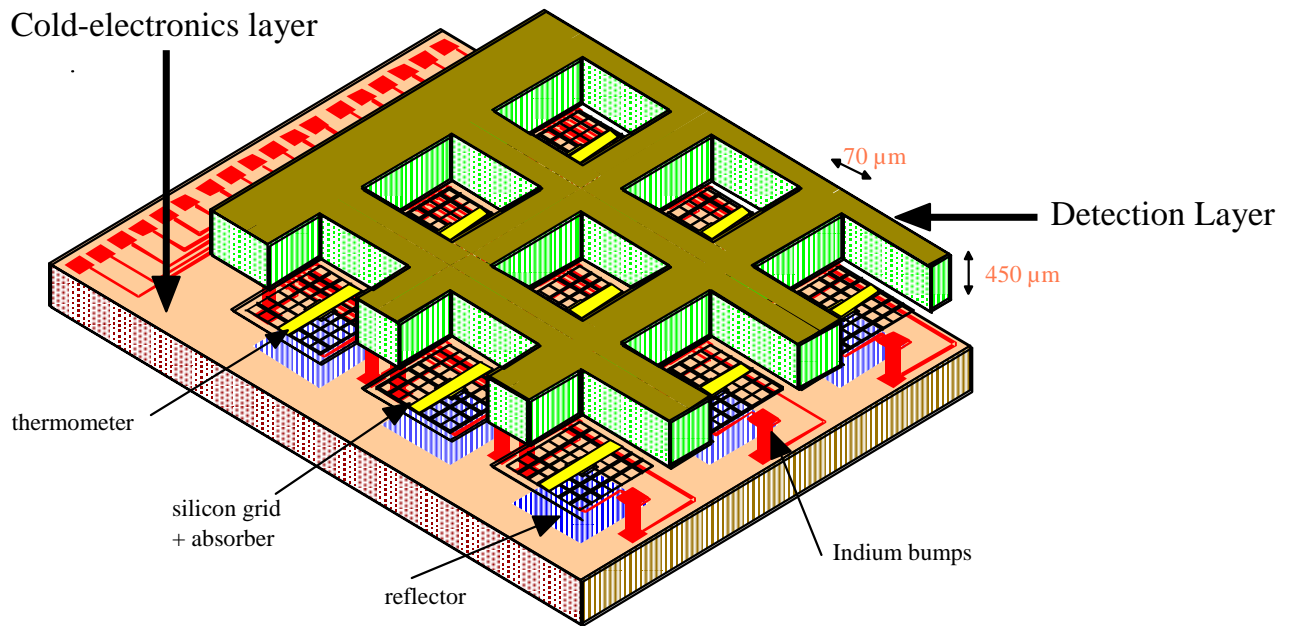


Figure 4: schematic drawing of the PACS bolometer array

The $450\mu\text{m}$ depth silicon substrate that supports these grids is hybridized on a second Si layer by indium bumps (Figure 4). The absorption efficiency profile can be adjusted beyond the $1/4$ wave cavity peak by suitable periodic grid patterns, adding a sort of 'horizontal resonance' through surface electromagnetic waves.

Each vertical cavity constitutes a single pixel of horizontal dimension $750\mu\text{m} \times 750\mu\text{m}$. This absorption principle results in arrays with a very large filling factor.

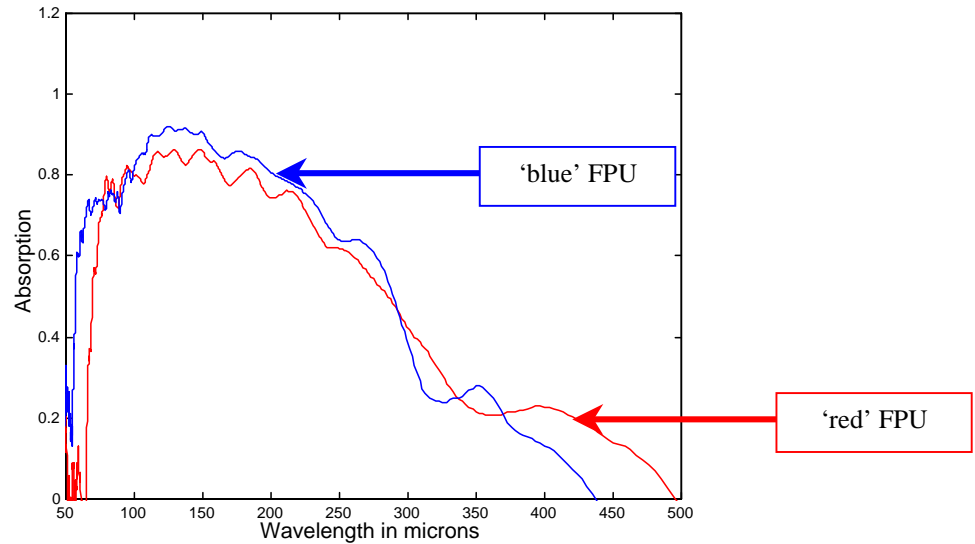


Figure 5: Absorption profile of the “blue” and "red" FPU

Recent measurements have shown that the ‘blue’ design ensures a satisfactory absorption profile for the two wavelength bands (Figure 5). Therefore, only one type of detector will be produced, that will help in improving the yield of the manufacturing process.

3. Sub-array of 18 x 16 pixels

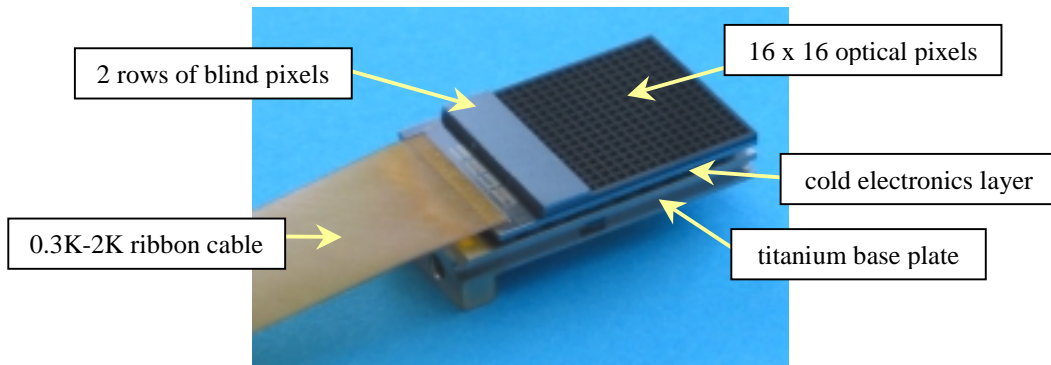


Figure 6: 16 x 18 pixels sub-array

The detector array is composed of sub-arrays of 16 rows x 16 columns active pixels (Figure 6). The output of every pixel is the middle point of a resistor bridge constituted by the thermometer on the pixel and a charge resistor located on the inter-pixel wall (70 μm wide). The charge resistor is identical to the thermometer (doping and geometry) but maintained at the heat sink temperature ($<300\text{mK}$). Two rows of blind pixels complete the sub unit geometry. These blind pixels are identical to the active pixels with two exceptions: a metallic opercula covers the top of these pixels, and a resistor (Figure 8) is added to simulate the incident optical power received by the active pixels. This additional resistor is also mounted in a bridge configuration to prevent any runaway current effect (Figure 7).

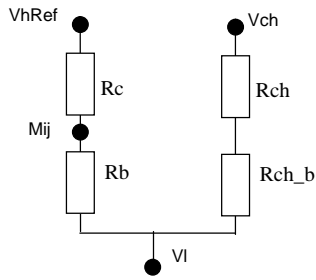


Figure 7: blind pixel thermometer bridges

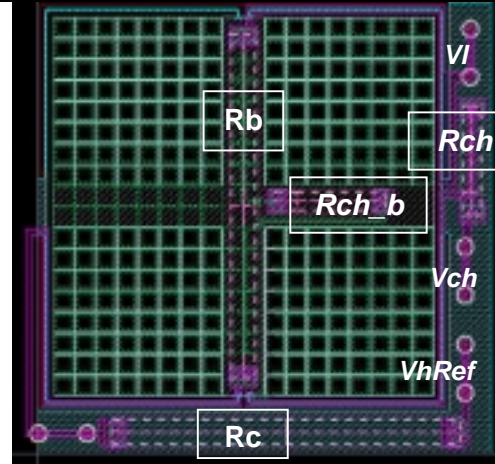


Figure 8: blind pixel layout

4. 300 mK electronics first stage (SMD)

Two main constraints are acting upon the electronics design:

- The high impedance of the thermometers makes the detector very sensitive to parasitic radio interferences.
- The band pass compatibility with the readout frequency, including the multiplexing -namely 1,5 kHz for the PACS bolometers- requires the use of very low capacitance lines between the thermometers' bridge and the first stage of amplification.

Therefore, the first stage of cascaded impedance adaptor CMOS circuit (refer to Figure 9) is implanted directly below the detection layer just under the cavity reflector, electrically connected to the bolometer resistors by the indium bumps. The middle point of the detector resistor bridge is connected to the gate of the PMOS readout transistor in a simple follower configuration. The stability of the current injected in this transistor is obtained by a second PMOS transistor mounted in a current source configuration. This circuit includes also the $16 \rightarrow 1$ multiplexing function. This unique feature in the large arrays photometer domain makes possible the simultaneous reading of 16×10 pixels and thus the reduction of the electronic lines.

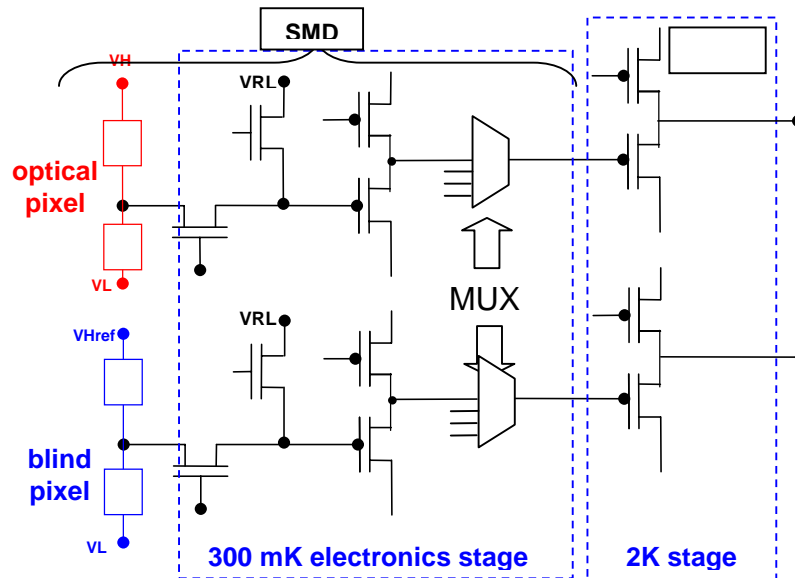


Figure 9: 300 mK & 2K circuit CMOS stages

In addition to the follower and “mux” functions, a specific double correlated sampling (DCS) functional mode has been introduced at the follower input. This DCS function consists of switching between a reference voltage VRL (Figure 9) and the bolometer mid-point voltage. Its role is to overcome the slow drift of the DC level of cold MOS transistor, which shows up as 1/f noise in the detector signal.

The assembly of these 2 layers, one for the detection of the incoming radiation and one for the cavity reflector and cold electronics, constitutes the Detection Sub-Modules (SMD) (Figure 9). They are thermally connected to the 300 mK cold finger of the ^3He sorption cooler through a titanium base plate and a copper strap.

5. 2K electronics stage (SMB)

A second stage of amplification, called a Buffer Sub-Module (SMB), is provided by PMOS preamplifiers at 2 K (Figure 9). Each SMB is connected to two SMD through 51 lines ribbon cables. This 2K stage ensures differential measurements between optical and blind pixels signals. This differential mode (DN) rejects the external collective perturbation. The output of the SMB presents 104 lines.

By combining the 0.3K and 2K stages functions, the bolometer detectors offer five possible acquisition modes:

- Direct measurement of the mid-point voltage (N): no double correlated sampling
- Double Correlated Sampling (H), no differential,
- Differential with blind pixels (DN) , no DCS,
- Differential with blind pixels, with DCS (DH),
- Differential with reference voltage on blind pixels and DCS

6. Complete focal planes assembly

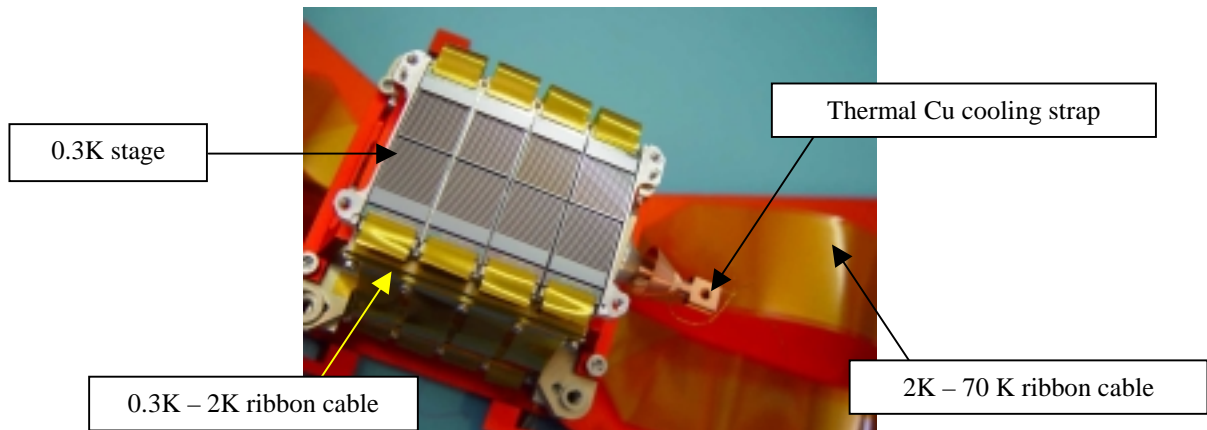


Figure 10: ‘blue’ focal plane unit

The PACS camera is composed of 2 focal plane units (FPU):

- one 60-130 μm ‘blue’ FPU made of 8 sub-arrays (2048 pixels) tiled together (Figure 10)
- one 130-210 μm ‘red’ FPU formed by 2 sub-arrays (512 pixels).

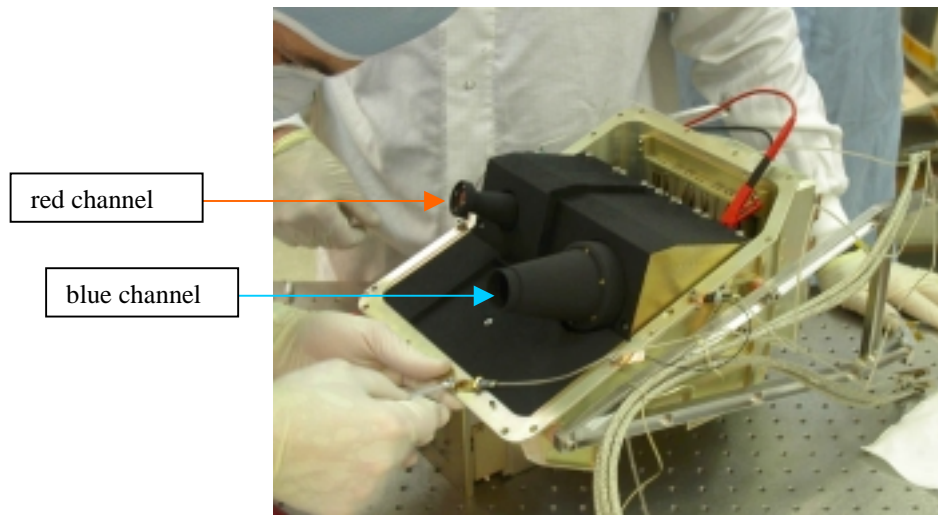


Figure 11: PACS focal planes

An Al common carrier that supports 8 (or 2) SMDs is mounted on a suspended structure from the 2 K level by Kevlar wires. The ribbon cables between the 300 mK and the 2 K stages are wrapped around the mechanical support and the 2K amplifier chips are screwed on a 2 K titanium common carrier. Two half-shells bolted to the mechanical support close the detectors' housing. Each detector unit is then ready to be mounted in the PACS Photometer assembly (Figure 11) which includes also the cryocooler, stray light baffles, optical filters and RF filters.

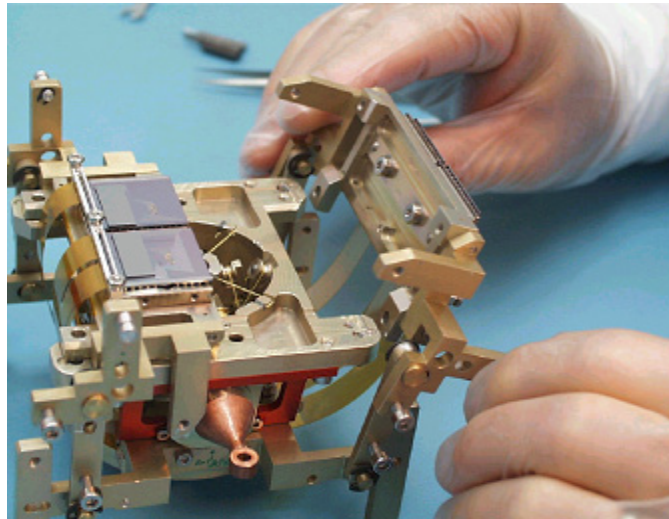


Figure 12: stage of the detector assembly

The manufacturing and the assembly of one focal plane (Figure 12) is a long and delicate process (ref. [6]) whose different steps are checked with numerous tests. During the assembly of the SMD and of the SMB, several tests (circuit outputs integrity, functional, ...) are done at room temperature.



Figure 13: individual tests of 4 SMDs placed inside the TriLir cryostat (here at 300K)

In particular, a test bench (Figure 13), developed in-house, performs an automatic test to check the inputs and outputs integrity, capacitance measurements and inter-lines insulations for up to 3×37 lines in a short time. This test is very relevant in regards to the great number of interconnections of the PACS camera. The FPU assembly requires 48 hybridization processes and 800 wire-bonding interconnections.

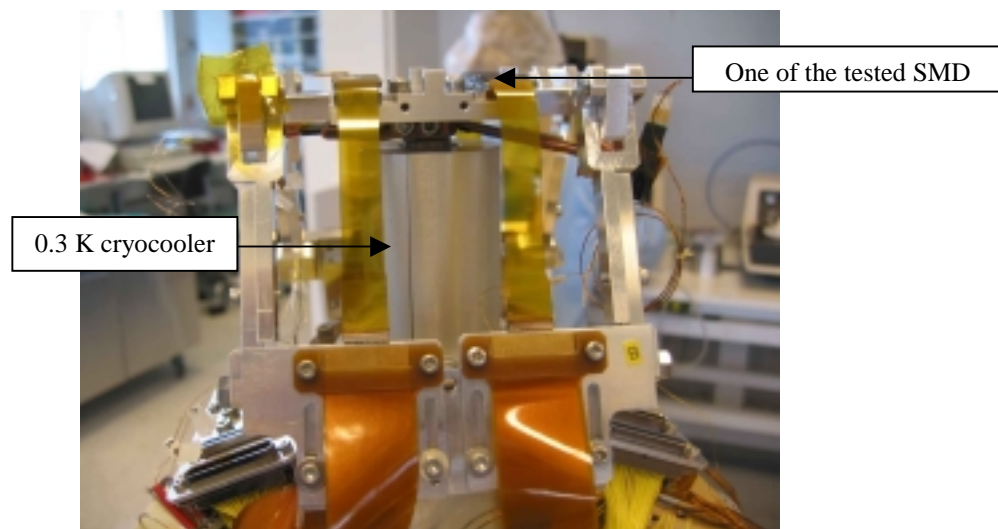


Figure 14: Setting up the sub-arrays in the 'TriLir' dewar test-bench

Before mounting the SMDs on a common carrier, we measure their electrical functionality and their electro-optical responses in a dedicated dewar ('TriLir', Figure 14). This new test-bench offers 2 main advantages. First, this test constitutes a very deep expertise of the thermal exchanges between the detection layer, the cold-electronics and the carrier. Second these 0.3K tests prevent mounting an abnormally over-dissipating SMD that would have 'polluted' its neighbouring SMD in a complete focal plane. Parasitic resistors, that are in some way hidden by the small resistances of the thermometers at 300K, are revealed at 300mK where thermometers resistances are very high: they may bring extra dissipated power that do not fit the specification of $1 \mu\text{W}$ maximum power per SMD. Moreover this test bench makes possible a first electro-optical response estimation.

CURRENT RESULTS

1. Qualification model FPU results

All measurements have been done with a frame frequency of 20 Hz. During electro-optical response measurements the black-body radiation is “chopped” between 0 and 1 pW (mean value). Salt filters are used to cut the blackbody spectrum below 85 μm in wavelength. Above this limit, the incident flux considered to extract the response is the total spectrum, without correction from the detector absorption details. The response is consequently underestimated.

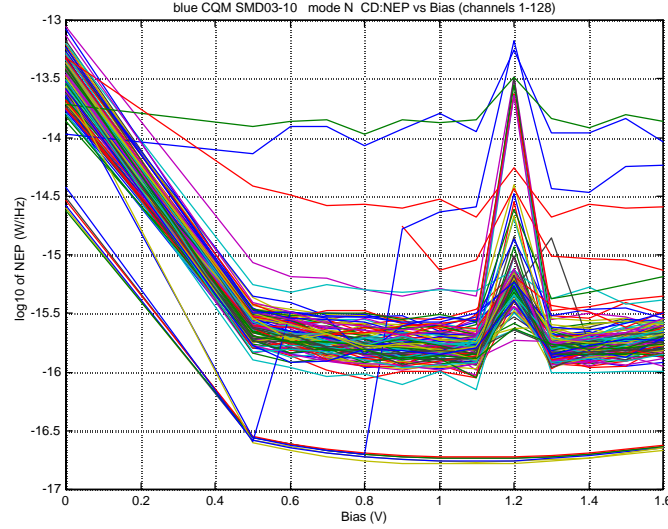


Figure 15: NEP vs. the voltage bias of one 16x16 array

During direct measurement, signal at the mid-point voltage is quite important: the responsivity reaches $7-8 \cdot 10^{10} \text{ V/W}$. Most pixels show a noise density centered around $10^{-5} \text{ V.Hz}^{-1/2}$. The detector achieves a mean NEP of $1.5 \cdot 10^{-16} \text{ W.Hz}^{-1/2}$, value very close to the required $1 \cdot 10^{-16} \text{ W.Hz}^{-1/2}$ (BLIP).

The NEP dispersion must be reduced firstly from an electro-thermal point of view by applying adapted voltage to the resistors added to each blind pixel. That way the blind pixels present the same thermal load as the one that the active optical pixels receive. Furthermore, the dispersion can be reduced by optimizing the 2K stage parameters in order to tune a unity gain to the followers.

When applying the nominal mode (Differential & DCS), the NEP should be degraded by a factor 2. We measure currently values around $3-5 \cdot 10^{-16} \text{ W.Hz}^{-1/2}$ showing an unexpected moderate excess. Since the 2K stage of electronics (SMB) shows a noise density of $0.5 \mu\text{V.Hz}^{-1/2}$ at 1Hz, and a $5 \cdot 10^{10} \text{ V/W}$ response, it does not limit the NEP. Noise limitations come today mainly from the 0.3K stage. Performances are expected to be improved :

- these results are extracted from raw data where correlated noise between pixels is not corrected
- flight model 0.3K electronics stages have lower noise.

2. Flight model focal plane units manufacturing

The Flight Model focal planes design differs from the Qualification ones in some items. The main differences between the QM FPU and FM FPUs are:

- Capacitances on electronic buses have been suppressed.
- All the thermometer polarizations plots are doubled and electrically connected.
- Protection diodes have been suppressed on specific outputs.
- The multiplexing NMOS transistor is replaced by a PMOS one (with its bulk connected to VDL).
- Optical pixels and blind pixels have separate high voltage polarizations (respectively V_h and V_{hRef}).

- A few tests functions are not any more available in the FM version circuit.

We are in the process of assembling a set of SMDs and SMBs. The present tests of SMDs within the TriLir cryostat at 0.3K make possible the pre-selection of the best components. They are currently assembled. Then complete electro-optics tests will be performed at 0.3K in Saclay on July 2004. The first flight model FPU will be delivered in the 4th quarter of 2004.

CONCLUSIONS

Present results are being carried out in accordance with the agreed plan.

Concerning the performances, electro-optical measurements have shown that this detector achieves a mean NEP of $1.5 \cdot 10^{-16} \text{ W.Hz}^{-1/2}$, value very close to the required $1 \cdot 10^{-16} \text{ W.Hz}^{-1/2}$ (BLIP). The NEP dispersion will be reduced from electro-thermal point of view by applying adapted voltage to the resistors added to each blind pixel. That way the blind pixels present the same thermal load as the one that the active optical pixels receive. Furthermore, the dispersion can be reduced by optimizing the 2K stage parameters in order to tune a unity gain to the followers.

The nominal mode (Differential & DCS) tests reveal values around $3\text{-}5 \cdot 10^{-16} \text{ W.Hz}^{-1/2}$ showing an unexpected moderate excess. Noise limitations come today mainly from the 0.3K stage that will be lessened because flight model 0.3K electronics stages have lower noise. Performances are also expected to be improved by applying signal processing to these raw data.

From the schedule point of view, a complete assembly (with 6 functional sub arrays out of 10) was delivered to the Max Planck Institute in April 2004 for integration in the QM instrument.

Flight Model focal planes are being produced at present time. Only one type of detector ('Blue' design) will be produced, that will help in improving the yield of the manufacturing process. The tests of detectors at 0.3K within a specific cryostat make possible the pre-selection of the best components. The selected ones are currently assembled and complete electro-optics tests will be performed at 0.3K in Saclay on July 2004. The first flight model FPU will be delivered in the 4th quarter of 2004.

REFERENCES

1. A. Potglitsch, C. Waelkens, N. Geis, *The Photodetector Array Camera and Spectrometer (PACS) for Herschel*, Proc. The Promise of the Herschel Space Observatory, 12-15 December 2000, Toledo, Spain, G.L. Pilbratt, J. Cernicharo, A.M. Heras, T. Prusti, R.A. Harris Edts. ESA publications, SP-460, page 29
2. M.J. Griffin, B.M. Swinyard, L. Vigroux: *The SPIRE instrument for Herschel*, Proc. The Promise of the Herschel Space Observatory, 12-15 December 2000, Toledo, Spain, G.L. Pilbratt, J. Cernicharo, A.M. Heras, T. Prusti, R.A. Harris Edts. ESA publications, SP-460, page 37
3. P. Agnèsè, L. Rodriguez et al. *Filled bolometer arrays for Herschel /PACS. in millimeter and submillimeter detectors for astronomy* T. G. Phillips & J. Zmuidzinas Editors SPIE proceedings Vol. 4855 (108-114) 2003
4. C. Cesarsky et al *ISOCAM in Flight*, A&A 315 (1996) L32
5. Hadley & Dennison JOSA 37 (1947)451
6. P. Agnèsè, J. Carcey, J.C. Cigna, C. Louis, J.L. Pornin, A. Vandenberghe and M. Volpert, *Compact 3D Packaging Of A Photodetector Array Camera And Spectrometer* IEE Nuclear Science Symposium, October 19-25 2003, Portland Or.